Phylogeny, morphology, and behavior of the new ciliate species *Stentor stipatus*

D. Rajan, B. Lee, A. Albright, E. Tang, A. Maravillas, C. Vargas, W. F. Marshall, D. Cortes

ABSTRACT

The study of evolution at the cellular level traditionally has focused on the evolution of metabolic pathways, endomembrane systems, and genomes, but there has been increasing interest in evolution of more complex cellular structures and behaviors, particularly in the eukaryotes. Ciliates have major advantages for such studies due to their easily visible surface patterning and their dramatic and complex behaviors that can be easily analyzed. Among the ciliates, the genus *Stentor* epitomizes the features that are useful for studying evolution: they are widespread in freshwater environments, easy to visualize because of their large size, and capable of complex behaviors such as learning, decision-making, and phototaxis.

Here, we introduce the discovery of a new species within this genus: *Stentor stipatus*, so named for their distinctive dark brown aggregates. We present morphological, phylogenetic, ecological, and behavioral characterizations of these cells. The *S. stipatus* clade has a bootstrap value of 93 and is phylogenetically distinct from *S. amethystinus*, the closest related species which shares a sequence similarity of 98.9%. *S. stipatus* is capable of phototaxis and can also habituate more quickly than *S. coeruleus*, the *Stentor* species in which most habituation studies have previously been conducted. These findings expand our understanding of *Stentor* species diversity, natural history, and demonstrate common principles of complex behavior that are present in single-celled organisms.

INTRODUCTION

The study of evolution at the cellular level has traditionally focused on the evolution of metabolic pathways and genomes, but there has been increasing interest in evolution of more complex cellular structures and behaviors, particularly in the eukaryotes. Ciliates (phylum Ciliophora) (Lee and Kugrens 1992) have major advantages for such studies due to their easily visible surface patterning and their dramatic and complex behaviors that can be easily analyzed. Moreover, ciliate biomass is a major component of aquatic ecosystems (Lischke et al. 2016) because ciliates are effective predators of smaller protists and bacteria, and also serve as an important food source for metazoa, providing a significant link between prokaryotic and eukaryotic food chains (Liu et al. 2016, Porter et al. 1979).

Among the ciliates, the genus *Stentor* epitomizes the features that are useful for studying evolution. *Stentor* is known for its trumpet-shaped morphology and large size, with some species visible to the naked eye (Tartar 1961, Slabodnick and Marshall 2014). The name *Stentor* references the Greek herald in the *Iliad* (Slabodnick and Marshall 2014) with a “voice as powerful as fifty voices of other men” (Homer), alluding to the cell’s trumpet shape. *Stentor*, like other members of the *Heterotrichae* class, are highly contractile and have a prominent membranellar band comprising long cilia around the oral cavity as well as shorter cilia distributed over the rest of the body (Tartar 1961).

Stentor species are widespread in freshwater environments (Foissner 1994, Reiff and Marshall 2015) and are notable for their easily visible surface patterning demarcated by pigmented stripes, their ability to perform complex behaviors, such as phototaxis (Kim et al. 1984), decision-making (Dexter et al. 2019), and learning (Rajan et al. 2023a) despite being unicellular, and thus lacking a nervous system. Furthermore, *Stentor* have the remarkable ability to regenerate after being injured by microsurgery (Morgan 1901, Tartar 1961). Studying *Stentor* thereby has the potential to reveal fundamental insights about cellular computation, wound healing, and development of complex morphology and behaviors.

A notable form of computation that *Stentor* exhibit is habituation, which is a form of learning characterized by a decrease in response after repeated stimulation. *Stentor* contract in response to mechanical stimulation, as an apparent escape response from predators in their natural pond habitat. However, after repeated stimulation, the *Stentor* cells habituate and thus stop contracting (Rajan et al. 2023a).

There are dozens of *Stentor* species, and all are characterized by trumpet-shaped morphology (Foissner et al. 1994). Some, like *S. amethystinus*, are smaller and more rounded, while others like *S. polymorphus* have a more elongated shape (Foissner et al. 1994). The *Stentor* genus also contains a variety of color patterns, including darkly pigmented species like *S. amethystinus* and *S. niger*, transparent species like *S. muelleri* and *S. roeselii*, and blue species like *S. coeruleus* and *S. multiformis* (Foissner et al. 1994). A few of these species, such as *S. roeselii* and *S. muelleri*, build lorica, which are mucilaginous structures surrounding the base of the cell into which the *Stentor* can contract (Foissner et al. 1994). Other species, like *S.*

pyriformis, are known to have algal endosymbionts (Hoshina et al. 2021). However, most work on *Stentor* has focused on *Stentor coeruleus*, while other members of the genus remain relatively unstudied. As a result, little is known about the natural history of *Stentor* as a whole or about the evolutionary relationships among the various *Stentor* species.

Here, we introduce the discovery of a new species within this genus: *Stentor stipatus*, so named for their distinctive dark brown aggregates. We present morphological, phylogenetic, ecological, and behavioral characterizations of these cells. These findings expand our understanding of *Stentor* species diversity, both in terms of their ecology and behavioral complexity, and highlight the importance of continued exploration to uncover hidden microbial biodiversity awaiting discovery in even well-studied ecosystems.

METHODS

Sample collection and culture

Stentor stipatus were collected from a white cedar swamp within the Two Ponds Conservation Area, near the edge of Sols Pond in Falmouth, Massachusetts (approximate coordinates of 41°33'52.0"N 70°36'26.9"W) continuously between early May and mid-July of 2023 and 2024. These *Stentor* were found readily amongst decaying plant matter in the acidic and iron-rich swampy shallows (Pregitzer 2015; www.mass.gov) that connect Sols and Jones ponds. Collection involved disturbing the topsoil underwater and scooping a portion of the suspended soil along with plant matter into small wide-mouth collection jars. Due to their heavy dark pigmentation, these *Stentor* were readily identifiable by the naked eye and could easily be isolated through use of a low-magnification SM2-TZ stereomicroscope (AmScope) with transillumination. *S. stipatus* cells were then isolated from these samples by use of a plastic dropper and placed into pasteurized pond water taken from a nearby pond (Morse Pond in Falmouth, Massachusetts) which is also iron-rich.

S. stipatus cells used for short-term phototaxis and action spectrum assays as well as for morphological characterization were grown in 100 ml wide-mouth jars, in indirect sunlight (on a windowsill that received around 10-12 hours of natural sunlight each day) at room temperature and were fed approximately 0.5 ml of *Chilomonas sp.* (Carolina Biologicals Cat. 131734) twice weekly. Under these conditions, *S. stipatus* cultures remained stable for approximately three months, while at the Marine Biological Laboratory in Woods Hole, Massachusetts.

The *Stentor* cells used for the habituation and long-term phototaxis experiments were grown in 6-well plates (Corning 353046) and cultured using a modified version of the protocol described in Lin et al. 2018. *Stentor* were fed from solid cultures of *Chlamydomonas* grown on Tris-Acetate-Phosphate (TAP) agar plates instead of liquid cultures as described in the aforementioned paper.

Morphological observations

General shape and size descriptions were made using data acquired on a Zeiss AxioZoom V.16 equipped with a PlanNeoFluar Z 2.3x/0.57 objective and a Thorlabs CS505CU 12-bit color

CMOS camera (Thorlabs). The scale for size measurements was established using a micrometer slide (AmScope) which was imaged at maximum magnification with the microscope set up as described.

Chilomonas culturing and *Stentor* feeding

Chilomonas sp. (Carolina Biologicals Cat. 131734) was grown in 100 ml wide-mouth jars in pasteurized pond water collected from a local pond (Morse Pond in Falmouth, Massachusetts). Cultures were seeded with 2-3 boiled wheat cherries to provide nourishment. Cultures were kept in the dark at 20 C and were checked regularly for any potential contaminants such as rotifers or other ciliates; contaminated cultures were disposed of. Stentor cultures were fed 0.5 ml of *Chilomonas* culture twice a week.

DNA extraction and amplification

Single cells were washed 3 times in pasteurized spring water (Carolina Biologicals Cat. 132458). DNA was isolated from these cells using a combination of worm lysis buffer (50 mM KCl, 10 mM Tris pH 8.2, 2.5 mM $MgCl_2$, 0.45% Igepal, 0.45% Tween 20, 0.01% gelatin) and proteinase K (New England Biologicals P8107) at a ratio of 166:1. Each *Stentor* cell was individually transferred in minimal volume into a tube containing 2.5 uL the worm lysis buffer + proteinase K. The tube was then placed in a -80^{o}C freezer for 10 minutes, and subsequently kept on ice. To complete the lysis, the samples were then heated at 60^{o}C for 60 minutes and then at 95^{o}C for 15 minutes.

For the polymerase chain reaction (PCR), a master mix solution was prepared containing 75 uL of Q5 High-Fidelity 2X Master Mix (New England Biologicals M0492S), 7.5 uL of the forward primer (5'-CAGCAGCCGCGGTAATTCC-3'), 7.5 uL of the reverse primer (5'-CCCGTGTTGAGTCAAATTAAGC-3'), and 45 uL of nuclease-free water (New England Biologicals B1500S). 22.5 uL of the master mix solution was then pipetted into each tube containing the lysed *Stentor*. PCR cycling parameters followed the conditions described in New England Biolabs 2022. Single band PCR products were confirmed using agarose gel electrophoresis, cleaned and concentrated (Zymo Research D4066), and then sent for Sanger sequencing.

Phylogenetic analysis

The NIH database codes used to identify 18S sequences for a range of different *Stentor* species were referenced from Taher et al. 2020, Fernandes et al. 2016, and Thamm et al. 2010. Alignments were generated using Clustal Omega (Madeira et al. 2024), subsequently trimmed with Phylogeny.fr Gblocks 0.91b (Dereeper and Guignon et al. 2008), and visualized with Jalview (Waterhouse et al. 2009). CLC Genomics Workbench (QIAGEN 24.0.1) was used to generate a phylogenetic tree from the cured alignment file, with *B. hyalinum* as the root node. The reliability of the branches was assessed using bootstrapping with 1000 replicates.

Habituation experiment

Habituation was assessed in the *Stentor cells* using a modified version of the protocol described in Rajan et al. 2023b. We used an Arduino-controlled habituation device to deliver mechanical taps to the cells at a specified force and frequency. We took videos of the cells over the course of the habituation experiment and quantified the fraction of cells contracted. A reduction in the proportion of cells that contracted over time indicated successful habituation, as the cells learned to ignore the mechanical stimulation. To improve video resolution, instead of using a USB microscope, the habituation device was placed directly on the stage of a dissection microscope (Zeiss Stemi 305) and an iphone camera was affixed directly to the microscope eyepiece. The 35 mm petri dish on the habituation device contained both *Stentor coeruleus* (VWR 470176-586) and *Stentor stipatus*, so that they could undergo the habituation training simultaneously. After 80 minutes of pretreatment with a level 4 pulse at a frequency of 1 tap/min, both species in the dish were then trained with level 3 pulses (higher force) at a frequency of 1 tap/min. Force levels are defined in Rajan et al. 2023b.

Phototaxis and action spectrum assays

Phototaxis was assessed in cells using modified versions of the protocols previously employed for other *Stentor* species (Kim et al. 1984). A custom 3D-printed chamber (Supp. Figure 1A) was made using high-clarity transparent resin (SirayaTech Blu V2). Following initial printing, the chamber was washed in 99% isopropanol for 5 minutes and then exposed to strong UV light for 30 minutes to remove residual resin and fully harden the structure. Following the long cure, the chamber was incubated at 60 C for 24 hours and soaked in pasteurized pond water overnight to remove any remaining volatile chemicals which may be detrimental to *Stentor* health. The chamber design featured a space, under the specimen area, into which a high powered LED (Chanzon) of specific wavelength can be inserted. Along the length of the specimen area, clear demarcation lines were added that split the long column into quadrants for easier quantification of phototaxis index (Figure S3).

For each experiment, between 100-200 *Stentor* cells were placed into the specimen area with enough water to fill this space up to half capacity (about 4 mm deep). The chamber, with *Stentor* cells, was then placed in a dark space on the stage of a dissecting stereomicroscope (AmScope SM2-TZ) and left in darkness for 1-2 minutes. For general phototaxis, a natural white LED, which covers a wide spectral band of light, was placed on one end of the chamber. For action spectrum analysis, LEDs of specific spectral wavelengths were used; these are [380nm, 410nm, 440nm, 460nm, 490 nm, 520 nm, 560 nm, 590 nm, 600 nm, 605nm, 625nm, 660 nm, 730 nm, and 850 nm]. After 1-2 minutes in darkness, the LED was lit just bright enough so as not to light up the opposite ‘dark’ end of the chamber, the brightness was modulated by altering the voltage fed to the LED with far red to orange LEDs generally requiring between 1.5-2.2 V and yellow to blue LEDs generally requiring between 2.2 - 3.2 V such that their Illumination (as measured using a lux meter held approximately 0.5 cm from the light source) ranged between 9,000 to 10,000 lux for all visible light LEDs and 500 to 1,000 lux for near IR and IR LEDs.

S. stipatus cells were then disturbed by pipetting and left for 5 minutes in the same dark space with the LED on. Next, the *Stentor* cells in each quadrant were counted by eye using the low magnification of the stereomicroscope. With most LEDs, Stentor cells could easily be counted without using the under-stage transmitted light of the stereomicroscope. For UV, red and far red LEDs, however, the stage transmitted light had to be turned on while counting.

Phototaxis was measured as a 'phototaxis index' by comparing the Stentor cells within the first (A, light) and fourth (D, dark) quadrants only (Supp. Figure 1C). Stentor cells in the middle two quadrants were assumed to be either indifferent or more weakly phototactic. This index was calculated as $P = (A - D) / (A + D)$. The strength of phototaxis was measured by comparing the total number of cells in A and D versus the total number of cells, $\sigma = (A + D) / (A + B + C + D)$. The action spectrum was thus constructed by comparing the phototaxis index and strength of phototaxis for *Stentor* cells exposed to the range of light wavelengths mentioned above. Counting of cells in each quadrant was achieved by taking a short video of each quadrant using a 12 megapixel AmScope color camera connected to the camera port of the stereo dissecting microscope via a 0.33x magnification lens (AmScope); a single still frame showing each full quadrant was then used to count the total number of *Stentor* cells within that quadrant.

Centrifugation of *S. stipatus*

Approximately 100 *S. stipatus* cells were pooled into a 1.5ml centrifuge tube in approximately 700 microliters of pasteurized pond water. *S. stipatus* were centrifuged in a tabletop microcentrifuge at 12.5x1000 RPM for 5 minutes. Following centrifugation, *Stentor* cells were allowed to recover for 1 minute before being transferred via dropper to an imaging chamber for microscopy.

RESULTS

Description of morphological characteristics

By transmitted light at low magnification, this *Stentor* presented with a dark brown pigmentation that appeared to fill the inner cytoplasm (Figure 1A, C). With oblique light or darkfield, a slight green pigmentation is visible in the cortical cytoplasm, distinct from the internal inclusion of dark brown materials which now appeared more like a reddish pigmentation (Figure 1B, D). This pigmentation seemed to concentrate around the presumptive macronucleus near the center of mass of the cell (Figure 1E), similar to the related *S. amethystinus*. At higher magnification, rows of pigment granules became visible (Figure 1F). At very high magnification it became apparent that the *Stentor* cells were full of microalgal cells (Figure S1A) which are extremely autofluorescent (Figure S1B). Closer inspection of the distribution of the algal cells revealed that they are densely packed cortically with few to none present in the internal cytoplasm (Movie S1); these cortically packed algae are uniformly distributed everywhere except the region around the membranelles of the *Stentor* cell (Movie S2, visible gap in Figure S1B).

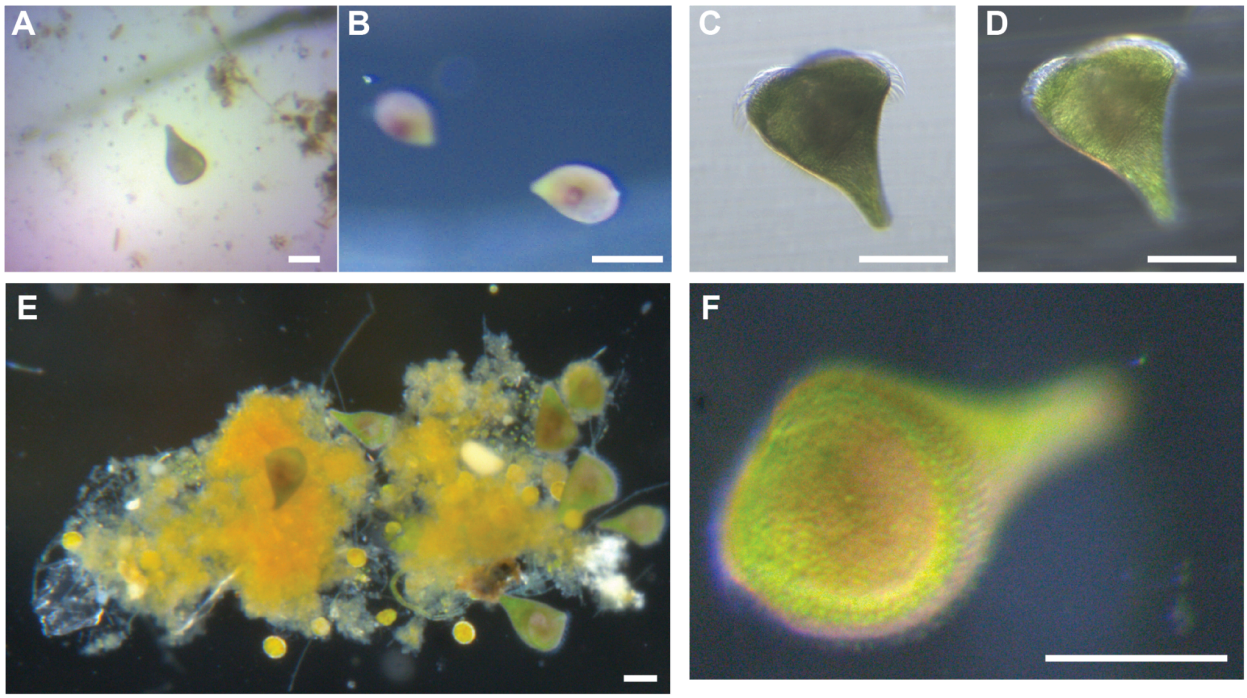

Figure 1. *Stentor stipatus* are densely packed with algae and pigment granules. A) At low magnification, *S. stipatus* cells look black and appear to have aggregate inclusion when imaged by transmitted light. B) At low magnification, *S. stipatus cells* demonstrate clear green and red pigmentation with dense aggregates of pigmentation located in the internal cytoplasm near their center of mass. C) Higher magnification transmitted light image showing how dark inclusion looks brown with the rest of the cell appearing more greenish. D) Same cell as in C, imaged via darkfield, showing the dark inclusion is the pigmentation. E) Low magnification image of a cluster of *S. stipatus* cells adhered to organic substrate. All cells have visible aggregate of pigmentation. F) Higher magnification darkfield image of a *S. stipatus* cell. Striations corresponding to bands of pigmentation are visible, reminiscent of the pigment granule banding seen in *S. coeruleus.* Scale bars equal 100 microns.

S. stipatus was found to be a very motile *Stentor* which attaches to substrate by its holdfast, but readily detaches and swims around with minimal perturbation. The motile shape of this stentor is tear drop-like with cells around 197±11.8 micrometers in length by 134±11.3 micrometers in width, with an aspect ratio of approximately 1.48±0.13 (n = 32; Figure S2A). At full extension, this *Stentor* did not change in shape much, with a slight decrease in aspect ratio to 1.4±0.2 (n = 35; Figure S2B) as cells appeared to expand slightly more in width than length. Fully extended, sessile *Stentor* had a large, flat frontal field, with membranelles exhibiting metachronal beating which was just visible by transmitted light with low magnification. Overall, this Stentor species exhibits limited expansion between swimming and sessile forms with statistically similar aspect ratios (Figure S2A, B), making it similar to *S. pyriformis* in this regard (Hoshina *et al.,* 2021). Upon contraction, cells withdrew their membranelles and shrank to an approximate aspect ratio of 1.0±0.1 (n = 11), nearly spherical in shape (Figure S2C).

Phylogenetic Analysis

Beyond morphological distinctions, the phylogenetic analysis based on 18S sequences revealed that *Stentor stipatus* is genetically distinct from other *Stentor* species (Figure 2). The bootstrap value of 93 indicates that *S. stipatus* is observed as a separate branch for 93% of the trials when the phylogenetic tree is regenerated 1000 times on resampled sets of data. *S. stipatus* has a 98.9% sequence similarity with *S. amethystinus*, the closest related species (Figure 2, Supp. File 1).

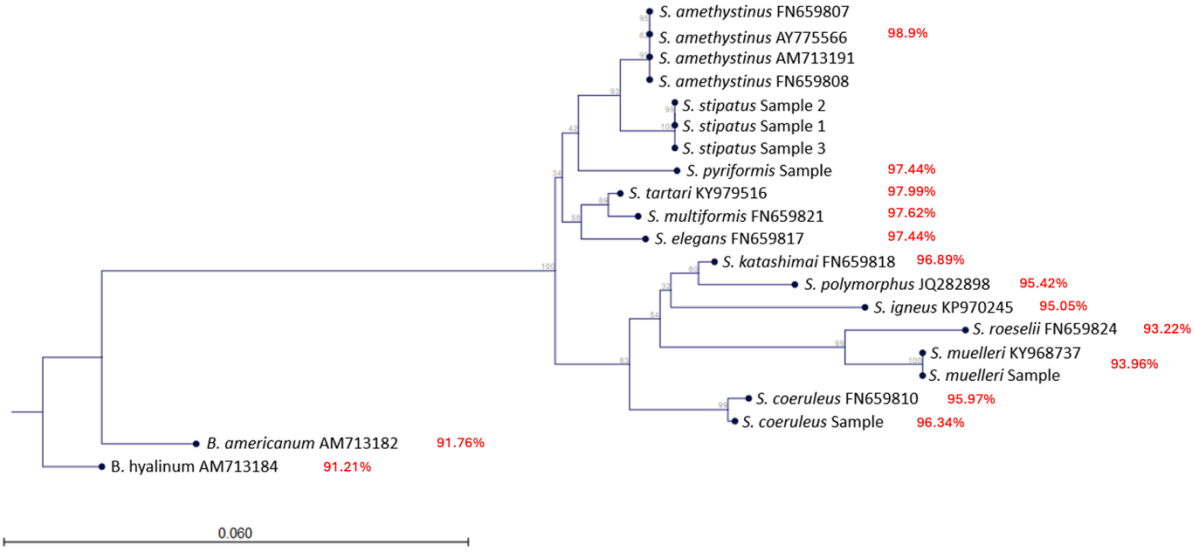

Figure 2. *Stentor stipatus* is phylogenetically distinct from other *Stentor* species. Scale bar indicates nucleotide substitutions per site. Percent similarities to *S. stipatus* are indicated in red. Newly sequenced cells are labeled with "Sample."

Habituation

Although many species distinctions are made on morphology and phylogeny alone, behavioral differences also capture essential information about the range of computational abilities present across a given genus. Indeed, we found that *S. stipatus* cells habituate more quickly compared to *S. coeruleus*. In previous experiments with *S. coeruleus* we employed four different force levels (Rajan et al. 2023b) with force level 1 being the strongest force (displacing the ruler on the habituation device by ~8 mm), to which *S. coeruleus* cells do not habituate over an hour-long experiment, and level 4 being the weakest (displacing the ruler on the habituation device by ~1 mm, with a downward peak force of ~0.288 N), which produces robust habituation in *S. coeruleus*.

When pretreated with level 4 pulses (lower force) for 80 minutes at a frequency of 1 tap / minute, 67% of the *S. stipatus* cells (n = 18) contracted in response to the first pulse while only 10% (n = 21) contracted in response to the final pulse. However, 100% of the *S. coeruleus* cells (n = 4) contracted throughout the entirety of the pretreatment period. When subsequently

given high force taps, the *S. stipatus* cells habituated within an hour (Figure 3). 67% of *S. stipatus* cells contracted in response to the first tap but only 22% of the cells contracted upon receiving the final stimulus. By contrast, 100% of *S. coeruleus* cells contracted in response to the first high force tap and none of these cells habituated within an hour.

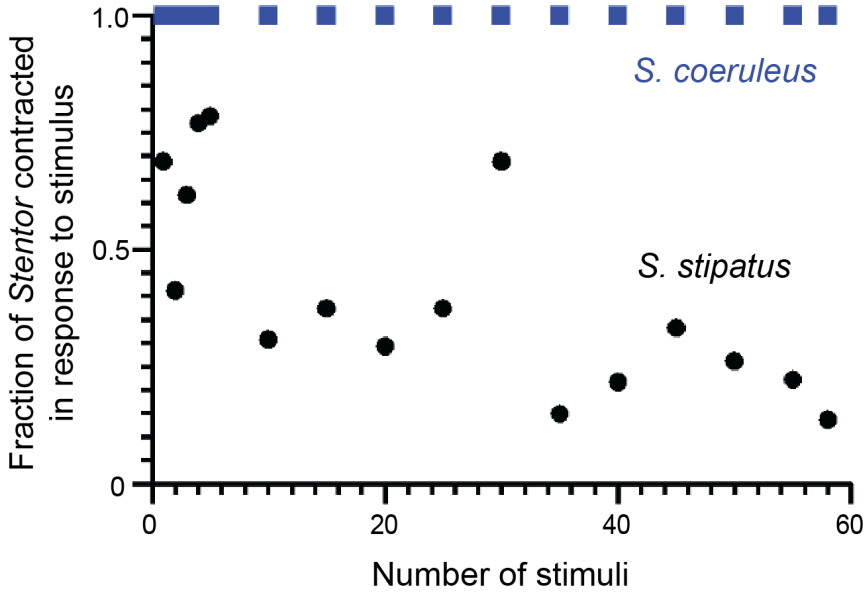

Figure 3. *S. stipatus* habituates more quickly to high force taps compared to *S. coeruleus*. Graph shows the habituation to mechanical stimulation of S. stipatus cells (n = 13-27) compared to the habituation of *S. coeruleus* cells (n = 4).

Action Spectrum analysis of *S. stipatus* reveals multiple phototaxis peaks

Besides habituation, phototaxis is another behavior that varies across the *Stentor* genus. On the short timescale, *S. stipatus* cells exhibited strong positive phototaxis when presented with asymmetric broadband white light or red-shifted light (380-840nm) light, with a phototaxis index of 0.75±0.23 (n = 3 experiments with a total of 413 cells) and 0.70±0.24 (n = 3 experiments with a total of 476 cells) respectively. The overall strength of this phototaxis (the percentage of total cells in either of the two extreme quadrants in our chamber) was measured at 75% for white light and 76% for red-shifted light.

Expanding our short timescale phototaxis to a range of specific wavelengths, we next explored the action spectrum of *S. stipatus*. Here we found positive phototaxis for all measured wavelengths with the phototaxis index varying between wavelengths. The phototactic response with highest phototactic index appeared to be around 590-600 nm and the weakest around 850 nm; a secondary, smaller peak in phototactic activity appeared under exposure to 520 nm light. A slight dip in activity around 490 nm also suggests a potential third, much less defined peak in the blue-green range of light around 430 nm (Figure 4).

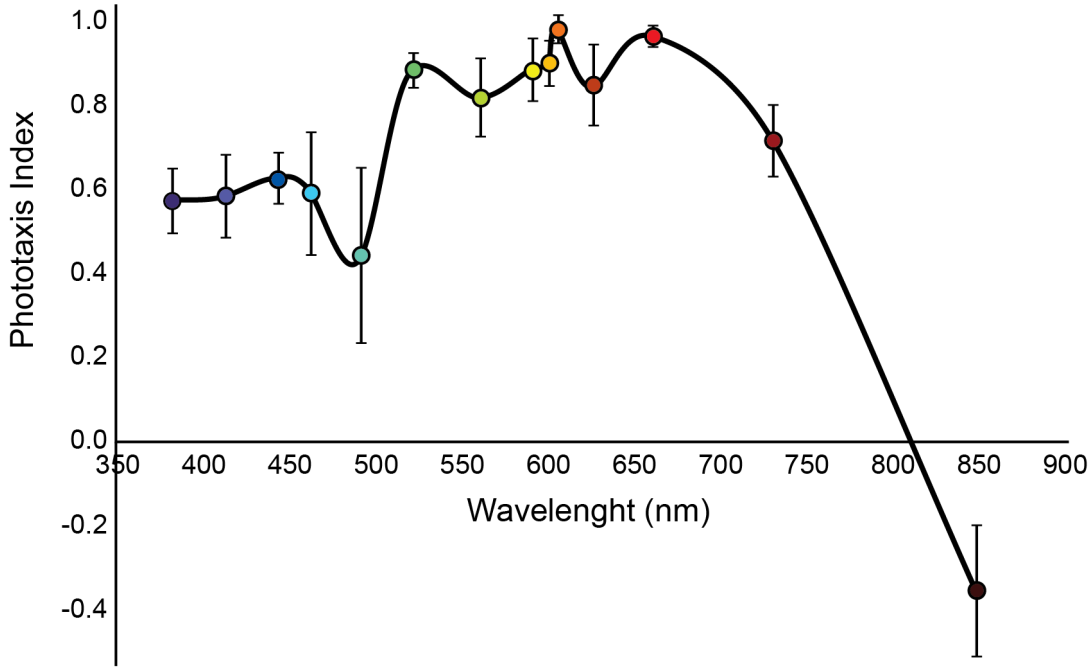

Figure 4. Action spectrum and phototaxis response of *S. stipatus*. Graph shows the phototaxis response of *S. stipatus* to different wavelengths of light ranging from ultraviolet (380 nm) to infrared (850 nm). For each experiment, between 100-200 cells were placed in the phototaxis chamber and counted; the experiment was repeated 4-5 times for each wavelength measured. Error bars are SEM.

Centrifugation of *S. stipatus* results in redistribution of dark pigmentation

Stentor pyriformis, which contains hundreds of endosymbiotic microalgae of genus *chlorella*, expels its microalgae following high-speed centrifugation (unpublished communication), after which *S. pyriformis* phototaxis is significantly reduced (unpublished results). Since *S. stipatus* demonstrates both dark pigmented inclusions along with peripheral green pigmentation (potentially denoting endosymbiotic photosynthesizers), we decided to test whether pigmentation or endosymbionts could be removed by centrifugation, and whether this would have an effect on the phototaxis demonstrated by these *Stentor*. Following centrifugation, *S. stipatus* demonstrated significant redistribution of dark pigmented inclusions such that half of the *Stentor* (divided along the long axis; Figure 5A) contained pigmentation while the other half was entirely transparent. In low light conditions, or with uniform light, these *Stentor* cells demonstrated no significant changes in morphology, behavior, or motility following centrifugation. If bright asymmetric light was applied to these *Stentor*, however, they exhibited altered swimming behavior; rather than swimming directly toward bright light, these *Stentor* cells swam in circles generating little effective movement (Movie S3, Figure 5A'). Over the course of about 10 minutes, the inclusions in these *Stentor* cells were seen to redistribute

such that they eventually fully covered the entire cell cytoplasm as before centrifugation (Movie S4, Figure 5B) and swimming became normal again (Movie S5).

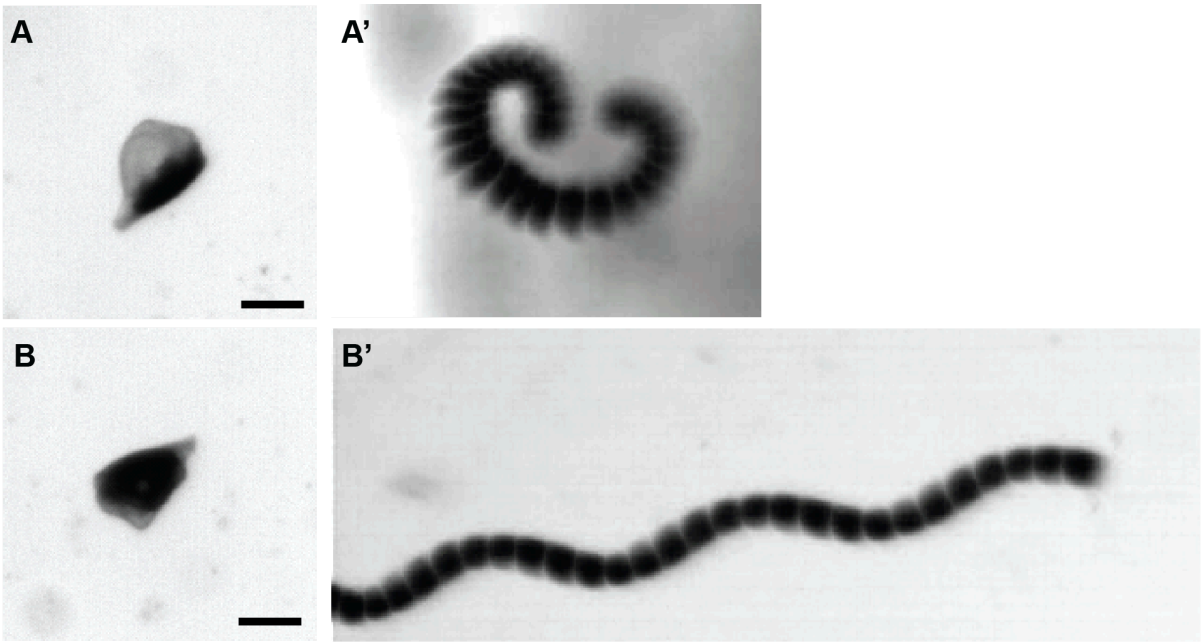

Figure 5. Effects of centrifugation on *Stentor* motility and light response. A) Close-up of *S. stipatus* cell following high-speed centrifugation. Dark pigmentation redistributes in a consistent left-right pattern shown in all assayed cells (n = 22). A') Time projection of swimming centrifuged *S. stipatus* cell. When presented with asymmetric light, these cells swim in a less progressive manner than normal (3/3). B) After seven to ten minutes of recovery, dark pigmentation is redistributed through the cell (n = 10). B') Time projection of centrifuged *S. stipatus* cell swimming after recovery. Following recovery of normal pigment distribution, cells now swim in the normal corkscrew pattern (3/3). Scale bars are 100 microns. Time projections are 28 frames from movies taken at 5 frames per second.

DISCUSSION

Here, we introduce *Stentor stipatus* as a new species based on our phylogenetic tree construction (Figure 2), which reveals an *S. stipatus* clade with a bootstrap value of 93 and shares a 98.9% sequence identity with the closest related species, *S. amethystinus*. The bootstrap value means that when the phylogenetic tree is regenerated 1000 times on resampled sets of data, *S. stipatus* is observed as a separate branch for 93% of the trials. Hillis and Bull 1993 established a widely used bootstrap threshold of 70 for considering a group of organisms as a distinct clade. This threshold has been employed in taxonomic categorizations across the tree of life, with examples in both invertebrate (Zhang et al. 2018) and vertebrate species (Spinks et al. 2009). Other taxonomic classifications of protists employ similar thresholds such as 75 (Zakrys 2024) or 60 (Slapeta 2005).

However, we also acknowledge the alternative possibility that *S. stipatus* is a divergent strain of *S. amethystinus* rather than a separate species, given that the bootstrap value is 93 and not 100. Charles Darwin wrote "It is good to have hair-splitters and lumpers" (Darwin 1857) in reference to the different attitudes of biologists towards taxonomy. The "splitters" emphasize the differences between organisms while the "lumpers" tend to prioritize similarities, resulting in broader species categorizations. Here, we fall under the category of "splitters" in our description of *S. stipatus* as a separate species. The closely related *S. amethystinus* is not reported to have the dark inclusions that we have observed in *S. stipatus*, but they are still in a comparable size range (Heep et al. 1998). Furthermore, both *S. stipatus* and *S. amethystinus* are less contractile (Figure 4, Cragg 1971) than other members of the *Stentor* genus– though this could be an artifact of their similar rounded morphology. Nevertheless, morphology alone is not an adequate identifier of *Stentor* species because *Stentor* morphology varies according to the region where conspecific cells were isolated (Heep et al. 1998).

To better differentiate between *S. stipatus* and *S. amethystinus*, we will need to obtain additional genetic material from both purported species for more detailed sequence comparisons. One limitation of taxonomical research on protists is inadequate environmental sampling and re-isolation (Adl et al. 2007), which can lead to a paucity of high-quality genetic material for phylogenetic comparisons, resulting in clades with low bootstrap values across the *Stentor* genus (Figure). Within the *Stentor* genus, the *S. amethystinus* clade is particularly disorganized due to variety in available sequences, and is sometimes not even considered monophyletic (Fernandes et al. 2016). Once additional isolates are gathered from field samples, molecular barcodes using specific genes can be used to distinguish between species more finely, as has been done in other protist genera such as *Tetrahymena* (Doerder 2019).

Many characterizations of new species focus on morphological descriptions (Foissner and Wölfl 1994), but our phototaxis and habituation experiments reveal that behavioral complexity is an essential feature of *S. stipatus* which can also distinguish it from other species. *S. stipatus* cells exhibit strong positive phototaxis over short timescales (Figure 4). Other *Stentor* species such as *Stentor pyriformis* exhibit positive phototaxis driven by the presence of endosymbionts, so differences in diets might affect phototaxis in *S. stipatus* as well. Future experiments will thus require adoption of standard culturing methods, something which is not yet possible as we work towards identifying ideal culturing conditions.

One interesting feature of habituation in *Stentor*, similar to habituation in animals, is that cells habituate more rapidly to weaker stimuli. The fact that *S. stipatus* cells appear to be less sensitive (i.e. a smaller fraction of untrained cells contract in response to a given mechanical stimulus) and also quicker to habituate (see Figure 3) may provide an opportunity to investigate the relation between sensitivity and habituation rates. For example, one concrete question is whether the habituation curve in *S. stipatus* matches the habituation curve seen in *S. coeruleus* when different forces are used in the two species that give the same initial contraction probability. *S. stipatus* might also be a convenient organism for long-term time lapse imaging because it is less likely to contract in response to extraneous vibrations under the

microscope. Genomic sequence comparisons among *Stentor* species might help to reveal the genetic basis for differences in mechanical sensitivity.

In the future, better characterization of *S. stipatus* will require collection of additional cells to sequence replicates, resulting in a more nuanced phylogenetic tree construction. Once we understand the optimal conditions for long-term *S. stipatus* culturing in the lab, we can also carry out replicates for phototaxis and habituation experiments. In particular, we can test the stimulus-specificity and force-specificity of habituation in *S. stipatus* to check if they match the patterns seen in wild-caught *S. coeruleus* cells, which can habituate to other non-mechanical stimuli such as light (Wood 1973). Furthermore, we can explore whether *S. stipatus* shares the ability of *S. coeruleus* to regenerate. Our preliminary investigation suggests that *S. stipatus* can regenerate after bisection, but this experiment was done with a single cell and requires follow-up with a larger sample size. Future bisection experiments will also help us isolate the dark brown aggregates within *S. stipatus*. Following isolation, we can determine the composition of these aggregates via mass spectrometry and by streaking out the contents on agar plates to check for the presence of endosymbionts. We can then compare the contents of these aggregates with the water composition of the native environment in which *S. stipatus* is found; we speculate that these inclusions may contain iron because the white cedar swamp in which these cells were found is iron-rich.

Our characterization of *S. stipatus* adds to our understanding of common principles of complex behavior that are present in single-celled organisms. Furthermore, our morphological and environmental descriptions contribute to our knowledge of protist natural history, which remains relatively understudied. Finally, since ciliate biomass is a major component of aquatic ecosystems, our exploration of ciliate diversity helps us understand the roles of complex cellular behavior in carving out ecological niches.

ACKNOWLEDGEMENTS

Initial discovery and collection of this novel *Stentor* species was made possible through funding by the Grass Foundation through the sponsorship of Daniel Cortes as a Grass Fellow in 2023. We also thank Mark Slabodnick for guidance on phylogenetic analysis. Molecular analysis was performed in the CCC Summer Course supported by NSF grant DBI-1548297 and NIH 5K12GM081266. Experiments on *S. stipatus* habituation were supported by NIH grant R35GM130327 and work on the phylogeny of wild Stentor species was supported by a grant from the Moore Foundation.

REFERENCES

Adl, Sina M., et al. “Diversity, Nomenclature, and Taxonomy of Protists.” Systematic Biology, edited by Tim Collins and Jack Sullivan, vol. 56, no. 4, Aug. 2007, pp. 684–89. DOI.org (Crossref), https://doi.org/10.1080/10635150701494127.

Cragg, Paul R. “An Explanation for the Limited Contractility of Stentor Amethystinus Leidy, 1880.” The Journal of Protozoology, vol. 18, no. 4, Nov. 1971, pp. 672–76. DOI.org (Crossref), https://doi.org/10.1111/j.1550-7408.1971.tb03395.x.

Darwin, Charles (1 August 1857). "Letter no. 2130". Darwin Correspondence Project. https://www.darwinproject.ac.uk/letter/DCP-LETT-2130.xml

Dereeper, Alexis and Guignon, Valentin et al. “Phylogeny.fr: robust phylogenetic analysis for the non-specialist.” Nucleic Acids Res. 2008 Jul 1;36(Web Server issue):W465-9. doi: 10.1093/nar/gkn180. Epub 2008 Apr 19. PMID: 18424797; PMCID: PMC2447785.

Dexter, Joseph P., et al. “A Complex Hierarchy of Avoidance Behaviors in a Single-Cell Eukaryote.” Current Biology, vol. 29, no. 24, Dec. 2019, pp. 4323-4329.e2. DOI.org (Crossref), https://doi.org/10.1016/j.cub.2019.10.059.

Doerder, F. Paul. “Barcodes Reveal 48 New Species of Tetrahymena , Dexiostoma , and Glaucoma : Phylogeny, Ecology, and Biogeography of New and Established Species.” Journal of Eukaryotic Microbiology, vol. 66, no. 1, Jan. 2019, pp. 182–208. DOI.org (Crossref), https://doi.org/10.1111/jeu.12642.

Fernandes, Noemi M., et al. “Expanded Phylogenetic Analyses of the Class Heterotrichea (Ciliophora, Postciliodesmatophora) Using Five Molecular Markers and Morphological Data.” Molecular Phylogenetics and Evolution, vol. 95, Feb. 2016, pp. 229–46. DOI.org (Crossref), https://doi.org/10.1016/j.ympev.2015.10.030.

Foissner, Wilhelm, and Stefan Wolfl. “Revision of the Genus Stentor Oken (Protozoa, Ciliophora) and Description of S.Araucanus Nov. Spec, from South American Lakes.” Journal of Plankton Research, vol. 16, no. 3, Mar. 1994, pp. 255–89, https://doi.org/https://doi.org/10.1093/plankt/16.3.255.

Heep, T., et al. “Stentor Amethystinus (Protista: Ciliophora: Heterotrichida), a Common Protozoan Member of Fresh-Water Plankton in Australia.” Records of the Australian Museum, vol. 50, no. 2, Oct. 1998, pp. 211–16. DOI.org (Crossref), https://doi.org/10.3853/j.0067-1975.50.1998.1280.

Hillis, D. M., and J. J. Bull. “An Empirical Test of Bootstrapping as a Method for Assessing Confidence in Phylogenetic Analysis.” Systematic Biology, vol. 42, no. 2, June 1993, pp. 182–92. DOI.org (Crossref), https://doi.org/10.1093/sysbio/42.2.182.

Homer, Iliad, Book 1, Line 1. http://www.perseus.tufts.edu/hopper/text?doc=Perseus:text:1999.01.0134. Accessed 6 May 2024.

Hoshina, R., Tsukii, Y., Harumoto, T., & Suzaki, T. “Characterization of a green Stentor with symbiotic algae growing in an extremely oligotrophic environment and storing large amounts of starch granules in its cytoplasm.” *Scientific Reports*, *11*(1). 2021. https://doi.org/10.1038/s41598-021-82416-9

Kim, I., et al. “Phototaxis and Photophobic Responses in Stentor Coeruleus Action Spectrum and Role of Ca2+ Fluxes.” Biochimica et Biophysica Acta (BBA) - General Subjects, vol. 799, no. 3, June 1984, pp. 298–304. DOI.org (Crossref), https://doi.org/10.1016/0304-4165(84)90274-5.

Lee, R. E., and P. Kugrens. “Relationship between the Flagellates and the Ciliates.” Microbiological Reviews, vol. 56, no. 4, Dec. 1992, pp. 529–42. DOI.org (Crossref), https://doi.org/10.1128/mr.56.4.529-542.1992.

Lin, Athena, et al. “Methods for the Study of Regeneration in Stentor.” Journal of Visualized Experiments, no. 136, June 2018, p. 57759. DOI.org (Crossref), https://doi.org/10.3791/57759.

Lischke, Betty, et al. “Large Biomass of Small Feeders: Ciliates May Dominate Herbivory in Eutrophic Lakes.” Journal of Plankton Research, vol. 38, no. 1, Jan. 2016, pp. 2–15. DOI.org (Crossref), https://doi.org/10.1093/plankt/fbv102.

Liu, Huaxue, et al. “Composition and Distribution of Planktonic Ciliates in the Southern South China Sea during Late Summer: Comparison between Surface and 75 m Deep Layer.” Journal of Ocean University of China, vol. 15, no. 1, Feb. 2016, pp. 171–76. DOI.org (Crossref), https://doi.org/10.1007/s11802-016-2712-7.

Madeira, Fabio et al. “The EMBL-EBI Job Dispatcher sequence analysis tools framework in 2024.” Nucleic Acids Research. 2024 Jul;52(W1):W521-W525. DOI: 10.1093/nar/gkae241. PMID: 38597606; PMCID: PMC11223882.

Morgan, Thomas Hunt. “Regeneration of proportionate structures in Stentor.” *Biol. Bull.* 1901; 2 311–328. 10.2307/1535709

New England Biolabs. “PCR with Q5® high-fidelity 2X master mix (M0492).” protocols.io. Feb. 2022. dx.doi.org/10.17504/protocols.io.bfkpjkvn

Porter, Karen G., et al. “Ciliate Protozoans as Links in Freshwater Planktonic Food Chains.” Nature, vol. 277, no. 5697, Feb. 1979, pp. 563–65. DOI.org (Crossref), https://doi.org/10.1038/277563a0.

QIAGEN CLC Genomics Workbench 24.0.1 (https://digitalinsights.qiagen.com/)

Rajan, Deepa, Tatyana Makushok, et al. “Single-Cell Analysis of Habituation in Stentor Coeruleus.” Current Biology, vol. 33, no. 2, Jan. 2023a, pp. 241-251.e4. DOI.org (Crossref), https://doi.org/10.1016/j.cub.2022.11.010.

Rajan, Deepa, Peter Chudinov, et al. “Studying Habituation in Stentor Coeruleus.” Journal of Visualized Experiments, no. 191, Jan. 2023b, p. 64692. DOI.org (Crossref), https://doi.org/10.3791/64692.

Reiff, Sarah B., and Wallace F. Marshall. “Stentor, Its Cell Biology and Development.” Encyclopedia of Life Sciences, by Wiley, 1st ed., Wiley, 2015, pp. 1–7. DOI.org (Crossref), https://doi.org/10.1002/9780470015902.a0025978.

Slabodnick, Mark M., and Wallace F. Marshall. “Stentor Coeruleus.” Current Biology, vol. 24, no. 17, Sept. 2014, pp. R783–84. DOI.org (Crossref), https://doi.org/10.1016/j.cub.2014.06.044.

Šlapeta, Jan, et al. “The Extent of Protist Diversity: Insights from Molecular Ecology of Freshwater Eukaryotes.” Proceedings of the Royal Society B: Biological Sciences, vol. 272, no. 1576, Oct. 2005, pp. 2073–81. DOI.org (Crossref), https://doi.org/10.1098/rspb.2005.3195.

Spinks, Phillip Q., et al. “Assessing What Is Needed to Resolve a Molecular Phylogeny: Simulations and Empirical Data from Emydid Turtles.” BMC Evolutionary Biology, vol. 9, no. 1, 2009, p. 56. DOI.org (Crossref), https://doi.org/10.1186/1471-2148-9-56.

Taher, Md Abu, et al. “Morphological Redescriptions and Molecular Phylogeny of Three Stentor Species (Ciliophora: Heterotrichea: Stentoridae) from Korea.” Zootaxa, vol. 4732, no. 3, Feb. 2020. DOI.org (Crossref), https://doi.org/10.11646/zootaxa.4732.3.6.

Tartar, Vance. The Biology of Stentor. Pergamon Press, 1961.

Thamm, Markus et al. “Insights into the Phylogeny of the Genus Stentor (Heterotrichea, Ciliophora) with Special Emphasis on the Evolution of the Macronucleus Based on SSU rDNA Data.” Acta Protozool. 49, 2010, 149-157. https://www.researchgate.net/publication/228350342_into_the_Phylogeny_of_the_Genus_Stentor_Heterotrichea_Ciliophora_with_Special_Emphasis_on_the_Evolution_of_the_Macronucleus_Based_on_SSU_rDNA_Data#full-text

Waterhouse, Andrew et al. "Jalview Version 2 - a multiple sequence alignment editor and analysis workbench." Bioinformatics 25 (9), Jan. 2009, 1189-1191 doi: 10.1093/bioinformatics/btp033

Wood, David C. “Parametric Studies of the Response Decrement Produced by Mechanical Stimuli in the Protozoan, Stentor Coeruleus.” Journal of Neurobiology, vol. 1, no. 3, Jan. 1969, pp. 345–60. DOI.org (Crossref), https://doi.org/10.1002/neu.480010309.

---. “Stimulus Specific Habituation in a Protozoan.” Physiology & Behavior, vol. 11, no. 3, Sept. 1973, pp. 349–54. DOI.org (Crossref), https://doi.org/10.1016/0031-9384(73)90011-5.

Zakryś, Bożena, et al. “Discovery of a New Photosynthetic Euglenoid in Poland: Euglena Mazurica Sp. Nov. (Euglenales, Euglenaceae).” Protist, vol. 175, no. 2, Apr. 2024, p. 126015. DOI.org (Crossref), https://doi.org/10.1016/j.protis.2024.126015.

Zhang, Shao-Qian, et al. “Evolutionary History of Coleoptera Revealed by Extensive Sampling of Genes and Species.” Nature Communications, vol. 9, no. 1, Jan. 2018, p. 205. DOI.org (Crossref), https://doi.org/10.1038/s41467-017-02644-4.